Coordination of Trivalent Metal Cations to Peptides: Results from IRMPD Spectroscopy and Theory

James S. Prell,[†] Tawnya G. Flick,[†] Jos Oomens,[‡] Giel Berden,[‡] and Evan R. Williams*,[†]

Department of Chemistry, University of California, Berkeley, California 94720-1460, FOM Institute for Plasma Physics "Rijnhuizen," Edisonbaan 14, 3439 MN Nieuwegein, The Netherlands

Received: September 29, 2009; Revised Manuscript Received: November 10, 2009

Structures of trivalent lanthanide metal cations La^{3+}, Ho^{3+}, and Eu^{3+} with deprotonated Ala_n ($n = 2-5$) or Leu-enk (Tyr-Gly-Gly-Phe-Leu) are investigated with infrared multiple photon dissociation (IRMPD) spectroscopy between 900 and 1850 cm^{-1} and theory. In all of these complexes, a salt bridge is formed in which the metal cation coordinates to the carboxylate group of the peptide, resulting in a limited conformational space and many sharp IRMPD spectral bands. The IRMPD spectra clearly indicate that all carbonyl groups solvate the metal cation in each of the Ala_n complexes. Due to strong vibrational coupling between the carbonyl groups, a sharp, high-energy amide I band due to in-phase stretching of all of the amide carbonyl groups bound to the metal cation is observed that is separated by $\sim$50 cm^{-1} from a strong, lower-energy amide I band. This extent of carbonyl coupling, which is sometimes observed in condensed-phase peptide and protein IR spectroscopy, has not been reported in IRMPD spectroscopy studies of other cationized peptide complexes. Intense bands due to carbonyl groups not associated with the metal cation are observed for Leu-enk complexes, indicating that a side chain group, such as the Tyr or Phe aromatic ring, prevents complete carbonyl coordination of the metal cation. Substitution of smaller lanthanide cations for La^{3+} in these peptide complexes results only in minor structural changes consistent with the change in metal cation size. These are the first IRMPD spectra reported for lanthanide metal cationized peptides, and comparison to previously reported protonated and alkali metal or alkaline earth metal cationized peptide complexes reveals many trends consistent with the higher charge state of the lanthanide cations.

Introduction

Many metal cations interact with a wide range of biomolecules and play important roles in a variety of biological processes. Coordination of metal cations with biomolecules can be highly specific, such as in potassium ion channels lined with carbonyl oxygen atoms spaced so as to solvate potassium much more efficiently than sodium, resulting in a dramatic selectivity for potassium conduction.[1] Planar arrangements of carbonyl oxygen atoms from partially unwound helices have been identified as part of a key motif in Ca^{2+} binding sites in some calcium pump-ATPases.[2]

The coordination of trivalent lanthanide metal cations to peptides and proteins is beginning to receive attention, and both the toxicity and potential therapeutic uses of these cations are being investigated.[3] Trivalent lanthanide metal cations can interfere with Ca^{2+} activity in vivo, blocking Ca^{2+} channels and disrupting Ca^{2+}-dependent enzymatic function.[3] X-ray crystallography structures of proteins in which La^{3+} substitutes for Ca^{2+} indicate coordination of La^{3+} by an average of 7.2 carbonyl oxygen atoms, whereas Ca^{2+} is typically 6-coordinate, and La^{3+} appears to have a greater tendency to form bidentate interactions with carboxylate groups than does Ca^{2+}.[4]

Despite the growing body of research concerning interactions of trivalent lanthanide cations with biomolecules,[3−13] detailed information about the coordination motifs of these ions and their preference for different functional groups is limited. Because electron-rich heteroatoms, such as nitrogen and oxygen, and aromatic groups can solvate charge, the structure of an ion−biomolecule complex and the mode of charge stabilization can be very sensitive to the identity of the charge carrier and biomolecule. Infrared multiple photon dissociation (IRMPD) spectroscopy is a powerful tool for investigating the structures of both isolated and hydrated ion−biomolecule complexes in the gas phase.[14] Using this technique, the relative stabilities of salt bridge and charge-solvated structures of metal cationized or protonated amino acids and small peptides as a function of gas-phase basicity[15−21] and acidity,[22] peptide sequence,[19,23] hydration state,[24] and metal ion size or charge state[15−19,23−34] have been studied for a variety of complexes.

The frequencies of vibrational modes for certain functional groups bound to metal cations often shift in a predictable manner due to the change in electron density and geometry of the functional group resulting from this interaction, and these frequency shifts can often be used to determine the binding motif of the metal cation. Carbonyl stretch frequencies are especially sensitive to metal cation binding or hydrogen bonding.[16−19,22,26−30,33,35] In complexes of di- and tripeptides with monovalent alkali and divalent alkaline earth metal cations, the amide carbonyl oxygen and carboxylate oxygen atoms (in salt bridge structures) often interact strongly with the metal cation, which can result in substantial frequency shifts for carbonyl stretch modes that correlate with metal ion charge state and size.[19,23]

For larger protonated and alkali metal or alkaline earth metal cationized peptides, on which only a few IRMPD spectroscopy studies in the carbonyl stretch region have been published,[23,31,36−43] the amide carbonyl stretch region can become congested as the

* Corresponding author. Phone: (510) 643-7161. Fax: (510) 642-7714. E-mail: williams@cchem.berkeley.edu.
[†] University of California.
[‡] FOM Institute for Plasma Physics.

10.1021/jp909366a
Published on Web 12/01/2009

TABLE 1: Electrospray Ionization Solution Conditions Used To Produce Precursor Ions

precursor ion	H_2O/MeOH ratio	metal salt (mM)	peptide (mM)
$(La•Ala_2 - H)^{2+}$	20/80	2.0	1.0
$(La•Ala_3 - H)^{2+}$	20/80	2.0	1.0
$(La•Ala_4 - H)^{2+}$	20/80	0.5	0.1
$(La•Ala_5 - H)^{2+}$	50/50	1.0	saturated
$(Ho•Ala_5 - H)^{2+}$	50/50	0.5	saturated
$(La•Leu\text{-}enk - H)^{2+}$	50/50	0.5	0.1
$(Eu•Leu\text{-}enk - H)^{2+}$	50/50	0.5	0.1

length of the peptide increases, making detailed interpretation of this region much more difficult. In solution, nearby amide carbonyl groups in peptides and proteins can couple together via through-bond and through-space interactions to yield carbonyl stretch vibrational signatures that can sometimes be used to identify secondary structures, such as helices, sheets, and turns.[44−47] Distinct bands associated with these vibrational signatures have yet to be reported for IRMPD spectra of cationized peptide complexes, although evidence for helical structures has been reported for protonated peptides on the basis of IR−UV double resonance spectra in the hydrogen-stretch region.[48−50]

We report here the IRMPD spectra of divalent lanthanide metal-peptide complexes $(La•Ala_n - H)^{2+}$ ($n = 2-5$), $(Ho•Ala_5 - H)^{2+}$, and $(M•Tyr\text{-}Gly\text{-}Gly\text{-}Phe\text{-}Leu - H)^{2+}$ (M = La and Eu), in the spectral region 900−1850 cm^{-1}. With the aid of hybrid density functional theory, metal cation coordination as a function of peptide length and metal cation size is investigated, as well as the role of aromatic side chains in coordinating trivalent metal cations.

Experimental Section

IRMPD Spectroscopy. IRMPD spectra were acquired using a 4.7 T Fourier-transform ion cyclotron resonance mass spectrometer coupled with a free electron laser (FELIX) that produces tunable infrared radiation. The instrument[51] and experimental methods[52] are discussed in detail elsewhere. Ions were produced by electrospray ionization from water/methanol solutions of Ala_n ($n = 2-5$) or Leu-enk (Tyr-Gly-Gly-Phe-Leu), and $LaCl_3$, $Ho(acetate)_3$, or $EuCl_3$ in the concentrations listed in Table 1. A solution infusion rate of 15 μL/min was used. All chemicals were obtained from Sigma-Aldrich, Steinheim, Germany, except Ala_4, which was synthesized at the University of Nijmegen. Stored waveform inverse Fourier transforms were used to isolate precursor ions, which were then irradiated for 4.5 s with tunable radiation from FELIX at a macropulse repetition rate of 5 Hz to produce extensive, but not complete, fragmentation of the precursor.

Computations. The La^{3+} ion is not implemented in available Monte Carlo molecular mechanics software; thus, low-energy structures of $(La•Ala_n - H)^{2+}$ were generated using the MMFFs force field as implemented in Macromodel 9.6 (Schrödinger, Inc., Portland, OR) and chemical intuition by first modeling $(Ca•Ala_n - H)^{1+}$. At least 10 000 structures were identified for each complex. Low-energy conformers were then divided into families with similar structures, and representative structures from each family were prepared for quantum mechanical geometry optimization in QChem v. 3.1[53] by direct substitution of La^{3+} for Ca^{2+}. Geometries of the resulting $(La•Ala_n - H)^{2+}$ structures were optimized with singlet electronic states at the B3LYP/6-31G* level of theory, using the CRENBL basis set and effective core potential for La. B3LYP/6-31G*/CRENBL structures for $(La•Tyr\text{-}Gly\text{-}Gly\text{-}Phe\text{-}Leu - H)^{2+}$ were obtained in an analogous method. Further geometry optimization of $(La•Ala_n - H)^{2+}$ structures was undertaken at the B3LYP/6-31+G(d,p)/CRENBL level of theory.

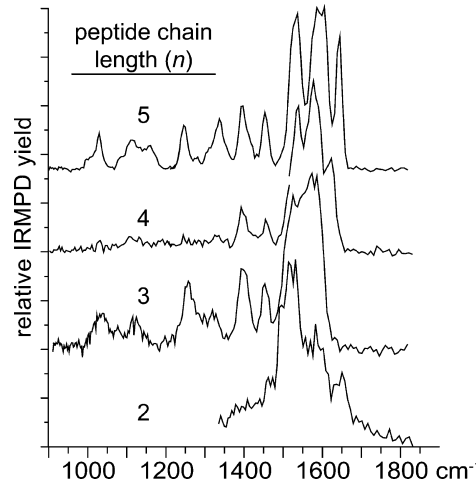

Figure 1. IRMPD spectra of $(La•Ala_n - H)^{2+}$, $n = 2-5$.

Each of the resulting $(La•Ala_n - H)^{2+}$ structures was found to have all real harmonic vibrational frequencies at this level of theory, indicating that they are local minima on the potential energy surface. Zero-point and 298 K enthalpies and entropies were calculated using unscaled harmonic vibrational frequencies, and 298 K Gibbs free energies were calculated using these enthalpies and entropies. Calculated infrared absorption spectra are plotted with frequencies scaled by 0.975, a scaling factor found to give reasonable agreement with experiment at this level of theory in many other studies,[16,17,19,20,22,26,31,35,54] and intensities are convolved with a 10 cm^{-1} Lorentzian profile to approximate experimental peak shapes.

Results and Discussion

IRMPD Spectra of $(La•Ala_n - H)^{2+}$ ($n = 2-5$). For the La^{3+}−polyalanine complexes investigated, $(La•Ala_n - H)^{2+}$ were the only metal-peptide ions observed in the electrospray ionization mass spectra. Formation of triply charged complexes of lanthanum with arginine-containing peptides of this size has been reported, where these ions are deprotonated at an acidic site and protonated at a basic site.[55] However, other studies suggest that as many as ∼21 residues may be necessary to form triply charged lanthanum−peptide complexes in the absence of arginine.[56] Displacement of a proton from a functional group other than a carboxylic acid has been reported by Pu et al. for singly charged Cr^{3+}−peptide complexes, although these authors conclude that deprotonation of the C-terminus is substantially more favorable.[57] It is therefore very likely that the C-terminus is deprotonated in these $(La•Ala_n - H)^{2+}$ complexes and that the trivalent metal cation interacts directly with the carboxylate group.

An IRMPD yield for each precursor was calculated from the intensities of the precursor (I_{prec}) and product (I_{prod}) ions measured after laser-induced fragmentation, corrected for the frequency-dependent laser power $P(\omega)$:

$$\text{IRMPD yield}(\omega) = (P(\omega))^{-1}(\Sigma I_{prod})/(I_{prec} + \Sigma I_{prod})$$

This IRMPD yield is plotted as a function of the laser frequency (ω) and normalized to the intensity of the most intense peak to obtain IRMPD spectra of the precursor species, which are shown in Figure 1. Due to the difficulty in forming $(La•Ala_2 - H)^{2+}$ and the limited FELIX time available, only a partial IRMPD

spectrum of this ion was obtained. The bands in these spectra are considerably narrower than those reported for alkali metal and alkaline earth metal cationized polyalanine peptides.[23,36]

Many of the bands in these IRMPD spectra can be assigned by comparison to condensed-phase IR spectra of polyalanine peptides as well as to IRMPD spectra of protonated or metalated Ala-containing peptides. In the region below 1500 cm^{-1}, a number of features are common to these spectra, suggesting that the functional groups contributing to these features are relatively insensitive to the chemical environment, or that their chemical environment changes little with the increasing length of the peptide. The sharp bands at ~1455 cm^{-1} in the spectra of $(La•Ala_n - H)^{2+}$ ($n = 3-5$) and the photodissociation observed there for $(La•Ala_2 - H)^{2+}$ are consistent with Ala side chain methyl CH bending modes, as observed in condensed-phase spectra of Ala-containing peptides[44] and IRMPD spectra of cationized Ala-containing peptides.[36,40,54,58] These modes, in particular, are rather insensitive to the chemical environment because they do not participate strongly in noncovalent interactions. The features observed near 1250 and 1330 cm^{-1} for $(La•Ala_n - H)^{2+}$ ($n = 3$ and 5) are consistent with bending motions of α-carbon CH bonds, which have been reported to occur in this region for many other Ala-containing peptides.[36,44] The absence or weakness of the ~1030 and ~1130 cm^{-1} modes in the spectrum of $(La•Ala_4 - H)^{2+}$ indicates that this ion has a different structural motif from those with $n = 3$ and 5, for which these bands are stronger.

There is a sharp band at ~1405 cm^{-1} for $n = 3-5$, where carboxylate symmetric stretch modes have been observed for many other complexes containing carboxylate groups.[27,28,32] This is consistent with deprotonation of the C-terminus for the complexes studied here, in which the resulting carboxylate group is expected to interact strongly with the metal cation. The frequency of the carboxylate symmetric stretch (s.s.) occurs very close to that of other amino acid−metal cation complexes in their salt bridge forms. In addition, the frequency of this mode does not vary substantially with increasing peptide chain length, even though coordination of additional carbonyl oxygen atoms to the metal in these complexes should result in partial charge transfer and, thus, a lower effective charge state of the metal ion. The insensitivity of the carboxylate s.s. frequency to chain length and interaction with a trivalent metal cation in these complexes is consistent with the previous observation that this frequency depends little on metal ion charge state.[27]

The region from 1500 to 1700 cm^{-1} contains several features that evolve with increasing peptide length. These features are considerably narrower than those observed in previously reported ambient temperature IRMPD spectra of alkali metal cationized or protonated polypeptides, likely due to stronger binding of the trivalent lanthanum cation to the carboxylate group, which limits the conformational space accessible at the temperature of the experiment. The sharp, intense band at ~1525 cm^{-1} in the spectrum of $(La•Ala_2 - H)^{2+}$ that gradually blueshifts to ~1550 cm^{-1} for $n = 3-5$ is consistent with the amide II (primarily NH in-plane bend) mode observed for *trans*-peptide moieties in condensed-phase IR spectra of polyalanine peptides[44] as well as IRMPD spectra of small polypeptide−metal cation complexes.[19,20,31,36−38,40,41,54] The carboxylate asymmetric stretch may also contribute intensity to this region.

A band at ~1585 cm^{-1} in the spectrum of $(La•Ala_2 - H)^{2+}$ gains in relative intensity and blue-shifts gradually to ~1600 cm^{-1} for $n = 3-5$ and can be attributed to the carboxylate asymmetric stretch or *trans*-amide I (primarily CO stretch) modes, which appear near this region for many peptide−metal cation complexes.[19,31,36,54,59] This feature is significantly redshifted relative to the amide I feature observed in alkali metal cationized peptides, consistent with stronger coordination of carbonyl oxygen atoms to the trivalent metal cation, resulting in greater partial charge transfer.[60,61] The blue shift of this mode with increasing peptide length is consistent with decreasing effective charge of the metal cation with increasing solvation by additional carbonyl oxygen atoms. Because the number of amide I and amide II modes is always equal for a given peptide length and increases with n, the roughly equal intensity of the two modes for $n = 3-5$ suggests that the unusually strong feature at 1520 cm^{-1} for $n = 2$ may be attributed in part to the carboxylate a.s., whose relative intensity in either the amide I or amide II region decreases with increasing peptide length.

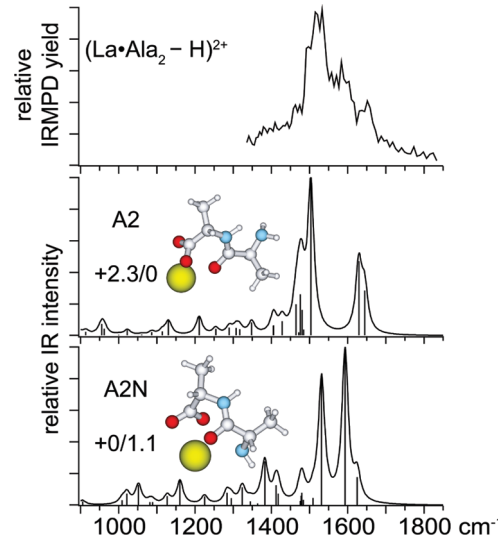

Figure 2. Experimental IRMPD spectrum and calculated structures and spectra with relative Gibbs free energies (kJ/mol) at 0/298 K for $(La•Ala_2 - H)^{2+}$.

The bands observed above ~1625 cm^{-1} in these spectra appear to be the most sensitive to peptide chain length, and their relatively high frequency indicates that they are due to carbonyl stretch or possibly N-terminal NH_2 scissor modes. These bands are assigned below on the basis of comparison to computed spectra and solution-phase IR spectroscopy of peptides.

Calculated Structures for $(La•Ala_n - H)^{2+}$ ($n = 2-5$). Representative low-energy structures calculated for $(La•Ala_n - H)^{2+}$ ($n = 2-5$) are shown in Figures 2−5, respectively, along with their calculated spectra and relative 0/298 K Gibbs free energies at the B3LYP/6-31+G(d,p)/CRENBL level of theory. Because the potential energy surface of each of these complexes is very large, only structures that significantly differ in their carbonyl−metal cation binding and peptide backbone dihedral motifs were investigated. No structures with cis peptide conformations were investigated, because such conformations should be sterically unfavorable for coordination of the metal cation to multiple amide groups in peptides of this size. Stable structures were found for each complex with the N-terminal nitrogen either stabilized by a hydrogen bond to an adjacent amide NH group (designated An) or solvating the metal cation (designated AnN), and for $n = 3$, two structures differing primarily in their peptide backbone dihedral angles were identified (A3N and A3N*).

In all of these structures, all oxygen atoms are found to coordinate the metal cation, consistent with a reported peptide carbonyl oxygen coordination number of ~8 for La^{3+}.[56] These structures also resemble those found to be low in energy for

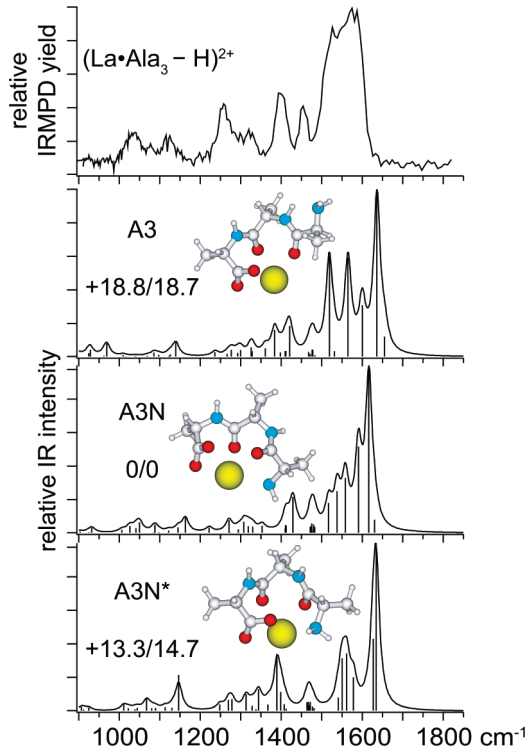

Figure 3. Experimental IRMPD spectrum and calculated structures and spectra with relative Gibbs free energies (kJ/mol) at 0/298 K for $(La•Ala_3 - H)^{2+}$.

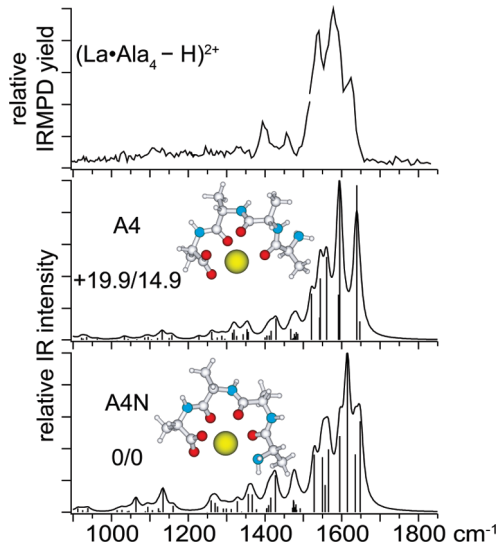

Figure 4. Experimental IRMPD spectrum and calculated structures and spectra with relative Gibbs free energies (kJ/mol) at 0/298 K for $(La•Ala_4 - H)^{2+}$.

sodiated di- and trialanine[36] and bariated trialanine.[23] Starting structures with amide oxygen atoms not interacting with the metal cation minimized to fully coordinated structures at the B3LYP/6-31G*/CRENBL level of theory. Numerous studies indicate that solvation of the metal cation by multiple heteroatoms in metal cationized peptides can result in greater stabilization as compared to structures in which charge solvation is less extensive, including some strongly dipole-stabilized salt bridge structures.[19,23,31,36,54,62−67] Carboxylate and amide carbonyl oxygen atoms as well as amine nitrogen atoms can be particularly effective at solvating charge in such complexes.

The energy difference between structures An and AnN increases with increasing length of the peptide chain. For n = 2, these structures are nearly isoenergetic, whereas for n = 5, the structure with the nitrogen solvating the metal cation is ~26/28 kJ/mol more stable at 0/298 K than the alternative structure in which this interaction does not occur. This trend is likely due to the less strained geometry of the peptide backbone possible for the larger complexes, which facilitates solvation of the metal by the N-terminal nitrogen atom. Binding of the N-terminal nitrogen and all carbonyl oxygen atoms to the metal is consistent with computational results for Co^{2+}-[59] and Cu^{2+}-bound[67] oligoglycines.

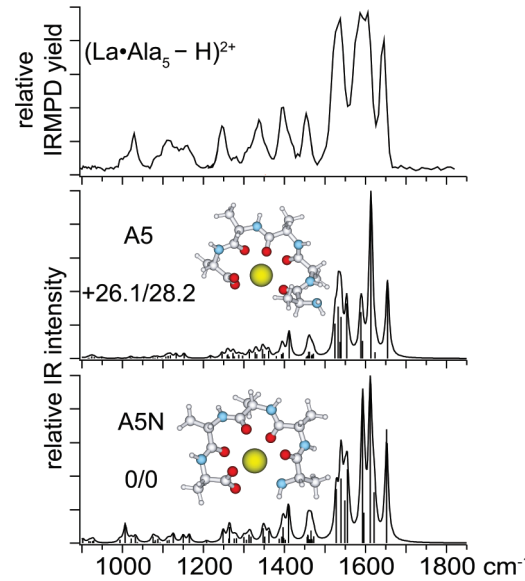

Figure 5. Experimental IRMPD spectrum and calculated structures and spectra with relative Gibbs free energies (kJ/mol) at 0/298 K for $(La•Ala_5 - H)^{2+}$.

On the basis of the dihedral angles of the peptide backbone in each of the structures identified, it is clear that coordination of the metal cation to all of the carbonyl oxygen atoms results in a peptide structure that is rather different from hairpin turns, helices, and sheet structures commonly observed in proteins. The dihedral angle pairs (φ, ψ) for these structures, where φ is the C′−N−C$^{\alpha}$−C′ angle and ψ is the N−C$^{\alpha}$−C′−N angle for a given residue, are approximately (55°, −170°) and (−55°, 170°), resulting in oxygen−oxygen distances that are much closer than those typical of α-, β-, γ-, and π-turns. This indicates that coordination of La^{3+} stabilizes conformations of the peptide that are otherwise unfavorable in the absence of the metal cation[44] or in protonated polyalanine and polyglycine peptides of comparable size.[39,40,42] For all structures identified, the peptide backbone C$^{\alpha}$ and N atoms lie roughly in a plane. The values of φ and ψ alternate in sign from one residue to the next in all but one structure (A3N*) so that the oxygen atoms coordinate the metal cation alternatingly from above and below this plane for all structures except A3N*. In structure A3N*, both amide carbonyl oxygen atoms coordinate the metal from the same side of this plane, which results in a ~13/15 kJ/mol higher energy at 0/298 K over the otherwise very similar structure A3N.

Comparison of Experimental and Calculated Spectra. The spectra of the lowest-energy structures identified for each complex provide reasonable agreement with the experimental spectra (Figures 2−5), suggesting that these or similar structures contribute substantially to the experimental ion population. In particular, the above assignments of spectral peaks to local modes are well-supported by the calculated spectra, which also aid in the assignment of other experimentally observed bands. No stable structures with free carbonyl oxygen atoms were

identified for any of these complexes; thus, it is unlikely that any of the bands in the experimental spectra originate from free amide carbonyl groups. For structure A2, the frequencies of the amine NH_2 scissor and amide I modes are considerably higher than in structure A2N. The experimental band at ~1585 cm^{-1} is thus attributable to a substantial ion population with the N-terminal nitrogen coordinated to the metal cation and the band at ~1650 cm^{-1} to a second large population without this coordination. The presence of both types of structures in the experimental ion population is in agreement with their similar calculated energies. For the larger peptide complexes studied, coordination of the metal cation to the N-terminal nitrogen is not calculated to result in as dramatic a frequency shift for the NH_2 scissor mode; thus, the presence or absence of a strong band above ~1625 cm^{-1} is likely attributable to other structural features. It is therefore also difficult to assess, on the basis of this feature alone, whether the N-terminal nitrogen is coordinated to the metal cation for $n = 3-5$, although calculated energies suggest this coordination occurs for all species investigated (vide supra). The band at ~1030 cm^{-1} for $n = 3-5$, discussed below, provides additional support for coordination of the N-terminal nitrogen.

It is known from condensed-phase studies of peptides and proteins and from IRMPD spectra of small protonated and alkali metal-cationized peptides that nearby amide I modes can couple to each other via both through-space and through-bond interactions, resulting in a symmetry-induced splitting of the amide I band into high- and low-energy regions.[31,44−47] Owing to their similar chemical environments and orientations toward the metal cation, the stretching motions of the amide carbonyl groups in all of these calculated structures (with $n = 3-5$) are, indeed, strongly coupled. The amide I mode in which all of the amide carbonyl groups stretch in-phase is calculated to have a significantly higher frequency than the other $(n - 1)$ amide I modes, and the frequency of this totally in-phase mode increases with n from ~1630 to ~1655 cm^{-1} for $n = 3-5$, in reasonable agreement with the experimental band that shifts from ~1590 to 1655 cm^{-1} for $n = 3-5$. As reported for other complexes,[36] this type of mode is very intense due to its large transition dipole moment. Both the frequency trend with n and the relative intensities calculated for this mode are in excellent agreement with the experimental spectra. The other coupled amide I modes are calculated to occur between 1580 and 1630 cm^{-1}, and the amide II and carboxylate asymmetric stretch modes occur between 1525 and 1575 cm^{-1}, also consistent with experiment.

Many very weak bands related to the N-terminal NH_2 rocking and wagging motions, CH bends, and other skeletal modes are calculated to occur below 1200 cm^{-1}, and these modes often couple strongly to each other. Of these modes, the strongest is associated with a nearly isolated NH_2 wag in the A*n*N structures, calculated to occur near 1030 cm^{-1}. The relatively high frequency of this mode, compared to free N-terminal NH_2 wag modes observed for other peptide complexes, can be attributed to its coordination to the metal cation, which increases the p-character of the nitrogen atom and, hence, the energy of this mode. There are some discrepancies in the intensities of the measured and calculated bands at frequencies below ~1200 cm^{-1}. Differences in relative intensities between IRMPD spectra and calculated absorption spectra can occur for a variety of reasons, including inaccuracies in calculated spectra and excitation-induced structural changes of the complex during the IRMPD process.[19,22,31]

These computational results and the experimental spectra strongly indicate that all oxygen atoms coordinate the metal cation in these complexes. Stable salt bridge structures of divalent alkaline earth metal cationized dialanine were recently reported on the basis of IRMPD spectroscopy results, whereas potassiated dialanine was found to adopt a nonzwitterionic structure.[23] In the salt bridge structures, which are stabilized in part due to the higher charge state of the metal ion, the amide carbonyl group was not bound to the metal cation but, instead, hydrogen-bonded to the protonated N-terminus. It is likely that, for $(La•Ala_n - H)^{2+}$, $n = 2-5$, which do not have a protonated N-terminus, structures without complete carbonyl oxygen coordination to the metal cation do not participate in compensatory hydrogen bonding, and such structures are therefore not observed.

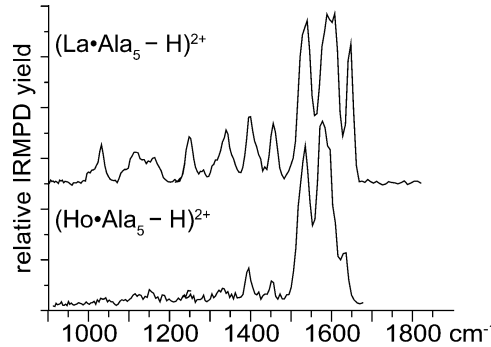

Figure 6. IRMPD spectra of $(La•Ala_5 - H)^{2+}$ and $(Ho•Ala_5 - H)^{2+}$.

Comparison of $(La•Ala_5 - H)^{2+}$ and $(Ho•Ala_5 - H)^{2+}$ IRMPD Spectra. The IRMPD spectra of $(La•Ala_5 - H)^{2+}$ and $(Ho•Ala_5 - H)^{2+}$ are shown in Figure 6. All of the strong spectral features described above for $(La•Ala_5 - H)^{2+}$ are also present when the La^{3+} cation is substituted with the smaller Ho^{3+} cation. However, for the Ho^{3+} complex, the lower- and higher-energy amide I bands are noticeably red-shifted by ~20 cm^{-1} (to 1580 and 1630 cm^{-1}, respectively), and the higher-energy amide I band is much weaker. These results are consistent with the smaller ionic radius of Ho^{3+}, as opposed to La^{3+} (0.901 vs 1.032 Å),[68] the former ion having a greater charge density and therefore causing a larger red shift in the stretch frequencies of attached carbonyls due to greater charge transfer.[60,61] This difference in metal ion size should enable the peptide to wrap further around Ho^{3+} so that the transition dipole moments of the outermost amide carbonyl groups more directly oppose each other, resulting in the observed weaker intensity of the higher-energy amide I mode and stronger intensity for the lower-energy amide I modes compared to those for the La^{3+} complex. The absence of a band near 1030 cm^{-1} and weakened intensity at 1630 cm^{-1} for the Ho^{3+} complex may also indicate that the N-terminal nitrogen does not coordinate the metal, consistent with a slightly more strained structure for the peptide in this complex.

IRMPD Spectra of $(La•Leu\text{-}enk - H)^{2+}$ and $(Eu•Leu\text{-}enk - H)^{2+}$. IRMPD spectra obtained for divalent complexes of the pentapeptide leucine-enkephalin (Tyr-Gly-Gly-Phe-Leu, "Leu-enk") with either La^{3+} or Eu^{3+} are shown in Figure 7. In contrast to the IRMPD spectrum reported for potassiated Leu-enk,[31] these spectra have many well-resolved bands. The 1500−1700 cm^{-1} region of these spectra is remarkably similar to those of $(La•Ala_{4,5} - H)^{2+}$, and no side chain groups of Leu-enk are expected to have strong bands in this region. The bands at ~1530 and 1580 cm^{-1} are thus attributable primarily to the amide II and lower-energy metal-bound amide I bands. The 1620 cm^{-1} band is likely the higher-energy metal-bound amide I band

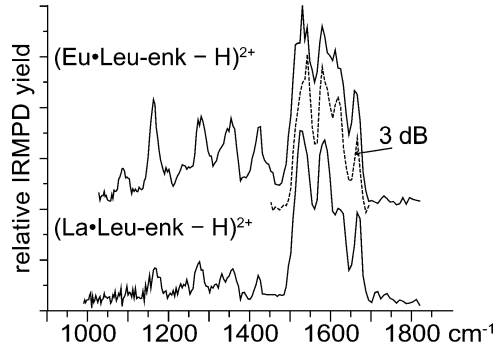

Figure 7. IRMPD spectra of $(La•Leu\text{-}enk - H)^{2+}$ and $(Eu•Leu\text{-}enk - H)^{2+}$, where Leu-enk = Tyr-Gly-Gly-Phe-Leu. The dotted line indicates the spectrum of $(Eu•Leu\text{-}enk - H)^{2+}$ obtained with 3 dB attenuation of the laser power.

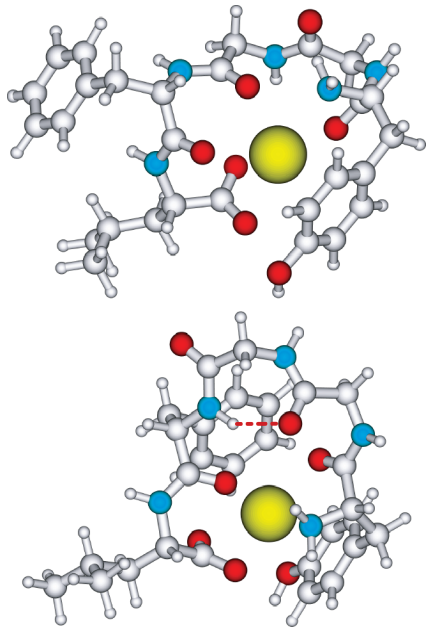

Figure 8. Representative low-energy B3LYP/6-31G*/CRENBL structures of $(La•Leu\text{-}enk - H)^{2+}$ in which aromatic side chains interact with the metal cation.

due to in-phase stretching of carbonyl groups and is more similar in frequency and relative intensity to that of $(La•Ala_4 - H)^{2+}$ rather than $(La•Ala_5 - H)^{2+}$ (vide supra). Thus, the effective charge of the metal cation is likely reduced relative to the pentaalanine complex, suggesting that fewer carbonyl groups solvate the metal cation in these Leu-enk complexes. Accordingly, the new band appearing at ~1660 cm^{-1} for both Leu-enk complexes is too high in frequency to be the stretch of a carbonyl group strongly bound to the metal cation and is, instead, consistent with the stretch of one or more free carbonyl groups.[69]

The π-electron system of aromatic side chain groups can interact strongly with metal cations in the gas phase, as observed for alkali and alkaline earth metal-cationized amino acids and small peptides.[23,29,31,34,52,54] The presence of free carbonyl groups in these two complexes likely results from the binding of an aromatic group or the Tyr side chain hydroxyl group to Eu^{3+} or La^{3+}. Two possible motifs for metal ion coordination by aromatic groups are shown in Figure 8, in which the Tyr and/or Phe side chain rings of Leu-enk effectively block several of the metal cation coordination sites and consequently displace carbonyl groups.

Conclusions

IRMPD spectroscopy is a powerful tool for understanding the coordination of metal cations to peptides. Attachment of trivalent metal ions to small peptides results in formation of deprotonated, doubly charged ions by ESI, where the metal cation displaces a proton at an acidic site. Investigating the structure of these ions has the advantage that these complexes have a salt bridge structure with a more limited conformational space than charge-solvated complexes in which the peptide itself is uncharged. The IRMPD spectra of these complexes contain many remarkably narrow bands due to the structural rigidity and limited conformational space of the complexes. For polyalanine complexes, spectral bands due to bending motions of the alanine side chains are found to be insensitive to peptide length, and the frequency of the carboxylate symmetric stretch mode is insensitive to both peptide length and effective charge of the metal cation. Both experiment and computations indicate that all carbonyl oxygen atoms coordinate to the metal ion for the polyalanine complexes and that the carbonyl groups couple to yield distinct higher-energy and lower-energy amide I bands separated by as much as 50 cm^{-1}. Coordination of the N-terminal amine nitrogen to the metal cation is found to be energetically favorable in each case. Changing the size of the lanthanide metal cation has only a mild spectroscopic effect for polyalanine complexes, consistent with a very minor change in structure. For Leu-enk, which contains two aromatic groups, the majority of the carbonyl oxygen atoms coordinate the metal cation, but at least one carbonyl group is displaced by an aromatic group coordinated to the metal cation, as suggested by low-energy calculated structures. Coupling of metal-bound amide carbonyl stretch modes is also observed for these Leu-enk complexes, again with a splitting of ~50 cm^{-1}.

These are the first IRMPD spectroscopy results for trivalent metal-cationized peptide complexes and the first evidence of well-resolved low- and high-energy metal-bound amide I bands resulting from carbonyl coupling. By measuring the IRMPD spectra of other complexes, it should be possible to determine spectroscopically the maximum carbonyl oxygen coordination number of trivalent lanthanide metal cations and to assess more thoroughly the competition between various functional groups to solvate the trivalent metal cation.

Acknowledgment. IRMPD spectra were acquired at the FOM Institute for Plasma Physics "Rijnhuizen," which is financially supported by the Nederlandse Organisatie voor Wetenschappelijk Onderzoek (NWO). The authors thank Prof. Wim van der Zande for the generous donation of Ala_4 and Drs. Britta Redlich and Anouk Rijs and the rest of the FELIX staff for excellent support. Generous financial support was provided by the National Science Foundation (Grants CHE-0718790 and OISE-730072).

Supporting Information Available: Full citation for ref 53. This material is available free of charge via the Internet at http://pubs.acs.org.

References and Notes

(1) MacKinnon, R. *Angew. Chem., Int. Ed.* **2004**, *43*, 4265–4277.
(2) Toyoshima, C.; Nakasako, M.; Nomura, H.; Ogawa, H. *Nature* **2000**, *405*, 647–655.
(3) Fricker, S. P. *Chem. Soc. Rev.* **2006**, *35*, 524–533.
(4) Pidcock, E.; Moore, G. R. *J. Biol. Inorg. Chem.* **2001**, *6*, 479–489.
(5) Lee, L.; Sykes, B. D. *Biochemistry* **1983**, *22*, 4366–4373.
(6) Bertini, I.; Janik, M. B. L.; Lee, Y. M.; Luchinat, C.; Rosato, A. *J. Am. Chem. Soc.* **2001**, *123*, 4181–4188.
(7) Ma, C.; Opella, S. J. *J. Magn. Reson.* **2000**, *146*, 381–384.

(8) Bertini, I.; Lee, Y. M.; Luchinat, C.; Piccioli, M.; Poggi, L. *ChemBioChem* **2001**, *2*, 550–558.
(9) Siedlecka, M.; Goch, G.; Ejchart, A.; Sticht, H.; Bierzyński, A. *Proc. Natl. Acad. Sci. U.S.A.* **1999**, *96*, 903–908.
(10) Fox, B. A.; Yee, V. C.; Pedersen, L. C.; Le Trong, I.; Bishop, P. D.; Stenkamp, R. E.; Teller, D. C. *J. Biol. Chem.* **1999**, *274*, 4917–4923.
(11) Burroughs, S. E.; Horrocks, W. D.; Ren, H.; Klee, C. B. *Biochemistry* **1994**, *33*, 10428–10436.
(12) Nitz, M.; Sherawat, M.; Franz, K. J.; Peisach, E.; Allen, K. N.; Imperiali, B. *Angew. Chem.-Int. Edit.* **2004**, *43*, 3682–3685.
(13) Chaudhuri, D.; Horrocks, W. D.; Amburgey, J. C.; Weber, D. J. *Biochemistry* **1997**, *36*, 9674–9680.
(14) Eyler, J. R. *Mass Spectrom. Rev.* **2009**, *28*, 448–467.
(15) Bush, M. F.; O'Brien, J. T.; Prell, J. S.; Saykally, R. J.; Williams, E. R. *J. Am. Chem. Soc.* **2007**, *129*, 1612–1622.
(16) Bush, M. F.; Forbes, M. W.; Jockusch, R. A.; Oomens, J.; Polfer, N. C.; Saykally, R. J.; Williams, E. R. *J. Phys. Chem. A* **2007**, *111*, 7753–7760.
(17) Bush, M. F.; Oomens, J.; Saykally, R. J.; Williams, E. R. *J. Phys. Chem. A* **2008**, *112*, 8578–8584.
(18) Forbes, M. W.; Bush, M. F.; Polfer, N. C.; Oomens, J.; Dunbar, R. C.; Williams, E. R.; Jockusch, R. A. *J. Phys. Chem. A* **2007**, *111*, 11759–11770.
(19) Prell, J. S.; Demireva, M.; Williams, E. R. *J. Am. Chem. Soc.* **2009**, *131*, 1232–1242.
(20) Prell, J. S.; O'Brien, J. T.; Steill, J. D.; Oomens, J.; Williams, E. R. *J. Am. Chem. Soc.* **2009**, *131*, 11442–11449.
(21) Drayss, M. K.; Blunk, D.; Oomens, J.; Gao, B.; Wyttenbach, T.; Bowers, M. T.; Schäfer, M. *J. Phys. Chem. A* **2009**, *113*, 9543–9550.
(22) O'Brien, J. T.; Prell, J. S.; Steill, J. D.; Oomens, J.; Williams, E. R. *J. Phys. Chem. A* **2008**, *112*, 10823–10830.
(23) Dunbar, R. C.; Steill, J. D.; Polfer, N. C.; Oomens, J. *J. Phys. Chem. B* **2009**, *113*, 10552–10554.
(24) Bush, M. F.; Prell, J. S.; Saykally, R. J.; Williams, E. R. *J. Am. Chem. Soc.* **2007**, *129*, 13544–13553.
(25) Drayss, M. K.; Blunk, D.; Oomens, J.; Schäfer, M. *J. Phys. Chem. A* **2008**, *112*, 11972–11974.
(26) Armentrout, P. B.; Rodgers, M. T.; Oomens, J.; Steill, J. D. *J. Phys. Chem. A* **2008**, *112*, 2248–2257.
(27) Bush, M. F.; Oomens, J.; Saykally, R. J.; Williams, E. R. *J. Am. Chem. Soc.* **2008**, *130*, 6463–6471.
(28) Dunbar, R. C.; Hopkinson, A. C.; Oomens, J.; Siu, C. K.; Siu, K. W. M.; Steill, J. D.; Verkerk, U. H.; Zhao, J. F. *J. Phys. Chem. B* **2009**, *113*, 10403–10408.
(29) Dunbar, R. C.; Polfer, N. C.; Oomens, J. *J. Am. Chem. Soc.* **2007**, *129*, 14562–14563.
(30) Heaton, A. L.; Bowman, V. N.; Oomens, J.; Steill, J. D.; Armentrout, P. B. *J. Phys. Chem. A* **2009**, *113*, 5519–5530.
(31) Polfer, N. C.; Paizs, B.; Snoek, L. C.; Compagnon, I.; Suhai, S.; Meijer, G.; von Helden, G.; Oomens, J. *J. Am. Chem. Soc.* **2005**, *127*, 8571–8579.
(32) Kapota, C.; Lemaire, J.; Maitre, P.; Ohanessian, G. *J. Am. Chem. Soc.* **2004**, *126*, 1836–1842.
(33) Polfer, N. C.; Oomens, J.; Dunbar, R. C. *Phys. Chem. Chem. Phys.* **2006**, *8*, 2744–2751.
(34) Dunbar, R. C.; Steill, J. D.; Polfer, N. C.; Oomens, J. *J. Phys. Chem. A* **2009**, *113*, 845–851.
(35) Rodgers, M. T.; Armentrout, P. B.; Oomens, J.; Steill, J. D. *J. Phys. Chem. A* **2008**, *112*, 2258–2267.
(36) Balaj, O. P.; Kapota, C.; Lemaire, J.; Ohanessian, G. *Int. J. Mass Spectrom.* **2008**, *269*, 196–209.
(37) Grégoire, G.; Gaigeot, M. P.; Marinica, D. C.; Lemaire, J.; Schermann, J. P.; Desfrançois, C. *Phys. Chem. Chem. Phys.* **2007**, *9*, 3082–3097.
(38) Polfer, N. C.; Oomens, J.; Suhai, S.; Paizs, B. *J. Am. Chem. Soc.* **2007**, *129*, 5887–5897.
(39) Vaden, T. D.; de Boer, T. S. J. A.; Simons, J. P.; Snoek, L. C.; Suhai, S.; Paizs, B. *J. Phys. Chem. A* **2008**, *112*, 4608–4616.
(40) Wu, R. H.; McMahon, T. B. *J. Am. Chem. Soc.* **2007**, *129*, 11312–11313.
(41) Wu, R. H.; McMahon, T. B. *J. Phys. Chem. B* **2009**, *113*, 8767–8775.
(42) Cimas, A.; Vaden, T. D.; de Boer, T. S. J. A.; Snoek, L. C.; Gaigeot, M. P. *J. Chem. Theory Comput.* **2009**, *5*, 1068–1078.
(43) Vaden, T. D.; de Boer, T. S. J. A.; Simons, J. P.; Snoek, L. C. *Phys. Chem. Chem. Phys.* **2008**, *10*, 1443–1447.
(44) Krimm, S.; Bandekar, J. *Adv. Protein Chem.* **1986**, *38*, 181–364, and references therein.
(45) Surewicz, W. K.; Mantsch, H. H.; Chapman, D. *Biochemistry* **1993**, *32*, 389–394.
(46) Torii, H. *J. Phys. Chem. B* **2008**, *112*, 8737–8743.
(47) Torii, H.; Tasumi, M. *J. Chem. Phys.* **1992**, *96*, 3379–3387.
(48) Stearns, J. A.; Boyarkin, O. V.; Rizzo, T. R. *Chimia* **2008**, *62*, 240–243.
(49) Stearns, J. A.; Boyarkin, O. V.; Rizzo, T. R. *J. Am. Chem. Soc.* **2007**, *129*, 13820–13821.
(50) Stearns, J. A.; Seaiby, C.; Boyarkin, O. V.; Rizzo, T. R. *Phys. Chem. Chem. Phys.* **2009**, *11*, 125–132.
(51) Valle, J. J.; Eyler, J. R.; Oomens, J.; Moore, D. T.; van der Meer, A. F. G.; von Helden, G.; Meijer, G.; Hendrickson, C. L.; Marshall, A. G.; Blakney, G. T. *Rev. Sci. Instrum.* **2005**, *76*, 023103.
(52) Polfer, N. C.; Oomens, J.; Moore, D. T.; von Helden, G.; Meijer, G.; Dunbar, R. C. *J. Am. Chem. Soc.* **2006**, *128*, 517–525.
(53) Shao, Y.; et al. *Phys. Chem. Chem. Phys.* **2006**, *8*, 3172–3191.
(54) Polfer, N. C.; Oomens, J.; Dunbar, R. C. *ChemPhysChem* **2008**, *9*, 579–589.
(55) Shi, T. J.; Siu, K. W. M.; Hopkinson, A. C. *J. Phys. Chem. A* **2007**, *111*, 11562–11571.
(56) Shvartsburg, A. A.; Jones, R. C. *J. Am. Soc. Mass Spectrom.* **2004**, *15*, 406–408.
(57) Pu, D.; Vincent, J. B.; Cassady, C. J. *J. Mass Spectrom.* **2008**, *43*, 773–781.
(58) Dunbar, R. C.; Steill, J. D.; Polfer, N. C.; Oomens, J. *Int. J. Mass Spectrom.* **2009**, *283*, 77–84.
(59) Constantino, E.; Rimola, A.; Sodupe, M.; Rodríguez-Santiago, L. *J. Phys. Chem. A* **2009**, *113*, 8883–8892.
(60) Velasquez, J.; Pillai, E. D.; Carnegie, P. D.; Duncan, M. A. *J. Phys. Chem. A* **2006**, *110*, 2325–2330.
(61) Zhang, G. Q.; Wang, W.; Chen, D. Z. *Chem. Phys.* **2009**, *359*, 40–44.
(62) Abirami, S.; Wong, C. H. S.; Tsang, C. W.; Ma, N. L.; Goh, N. K. *J. Mol. Struct. (THEOCHEM)* **2005**, *729*, 193–202.
(63) Teesch, L. M.; Adams, J. *J. Am. Chem. Soc.* **1990**, *112*, 4110–4120.
(64) Wong, C. H. S.; Ma, N. L.; Tsang, C. W. *Chem.—Eur. J.* **2002**, *8*, 4909–4918.
(65) Wyttenbach, T.; Bushnell, J. E.; Bowers, M. T. *J. Am. Chem. Soc.* **1998**, *120*, 5098–5103.
(66) Constantino, E.; Rimola, A.; Rodríguez-Santiago, L.; Sodupe, M. *New J. Chem.* **2005**, *29*, 1585–1593.
(67) Rimola, A.; Constantino, E.; Rodríguez-Santiago, L.; Sodupe, M. *J. Phys. Chem. A* **2008**, *112*, 3444–3453.
(68) Shannon, R. D.; Prewitt, C. T. *Acta Crystallogr., B* **1969**, *25*, 925–946.
(69) Constantino, E.; Rodriguez-Santiago, L.; Sodupe, M.; Tortajada, J. *J. Phys. Chem. A* **2005**, *109*, 224–230.

JP909366A